Supercritical fluid technology for the development of innovative ophthalmic medical devices: Drug loaded intraocular lenses to mitigate posterior capsule opacification

Kanjana Ongkasin, Yasmine Masmoudi, Christian Wertheimer, Anna Hillenmayer, Kirsten Eibl-Lindner, Elisabeth Badens

Version of Record: https://www.sciencedirect.com/science/article/pii/S0939641120300527
Manuscript_0ccb646c964467f730f16456b6ff58c4

Supercritical fluid technology for the development of innovative ophthalmic medical devices: Drug loaded intraocular lenses to mitigate posterior capsule opacification

Kanjana ONGKASIN[1], Yasmine MASMOUDI[1], Christian M. WERTHEIMER[2], Anna HILLENMAYER[2], Kirsten H. EIBL-LINDNER[2], Elisabeth BADENS[1]

[1]*Aix Marseille Univ, CNRS, Centrale Marseille, M2P2, Marseille, France*

[2]*Laboratory for Cell Biology, Department of Opthalmology, Ludwig-Maximilians-University, Munich, Germany*

Highlights

- Sustained release drug delivery intraocular lenses to prevent PCO
- Supercritical impregnation of methotrexate into intraocular lenses
- Efficient impregnation with sustained release of methotrexate over 80 days
- Epithelial cell morphology in loaded IOLs /fibroblastic phenotype in control IOLs
- Efficiency of methotrexate loading in preventing fibrosis involved in PCO

Abstract

Supercritical impregnation technology was applied to load acrylic intraocular lenses (IOLs) with methotrexate to produce a sustained drug delivery device to mitigate posterior capsule opacification. Drug release kinetics were studied *in vitro* and used to determine the drug loading. Loaded IOLs and control IOLs treated under the same operating conditions, but without drug, were implanted *ex vivo* in human donor capsular bags. The typical cell growth was observed and immunofluorescence staining of three common fibrosis markers, fibronectin, F-actin and α-smooth muscle actin was carried out. Transparent IOLs presenting a sustained release of methotrexate for more than 80 days were produced. Drug loading varying between 0.43 to 0.75 ± 0.03 $\mu g_{drug}.mg^{-1}_{IOL}$ were obtained when varying the supercritical impregnation pressure (8 and 25 MPa) and duration (30 and 240 min) at 308 K. The use of ethanol (5 mol%) as a co-solvent did not influence the impregnation efficiency and was even unfavorable at certain conditions. Even if the implantation of methotrexate loaded IOLs did not lead to a statistically significant variation in the duration required for a full cell coverage of the posterior capsule in the human capsular bag model, it was shown to reduce fibrosis by inhibiting epithelial-mesenchymal transformation. The innovative application presented has the potential to gain clinical relevance.

1 Introduction

Posterior capsule opacification (PCO) is the most common long-term complication after cataract surgery. The cataractous, cloudy lens can never be fully removed during surgery and lens epithelial cells remain in the capsular equator. These residual lens epithelial cells then

migrate and proliferate from the periphery, below the intraocular lenses (IOL) on the posterior capsule, towards the center into the optical axis [1–3]. Furthermore, they undergo epithelial to mesenchymal transformation resulting in a more fibroblastic phenotype which leads to contraction of the posterior capsule causing capsular wrinkling with increasing light scattering and a reduction in visual acuity [3–5]. Established risk factors are age, gender, dry eye disease, glaucoma, uveitis, age-related macular degeneration, hyperlipidemia [6], diabetic and inflammatory comorbidity [7], intraocular lens (IOL) design and material [8,9], surgical technique and surgeon experience [10].

Although IOL design (sharp-edge [11]), materials and surgical techniques have been significantly improved over the years [12], over long-term observation, PCO incidence remains frequent, and has to be treated by neodymium-doped yttrium aluminum garnet (Nd:YAG or $Nd:Y_3Al_5O_{12}$) laser capsulotomy [13,14]. The treatment completely disrupts the posterior capsule to clear the optical axis. Unfortunately, it cannot be used for all patients and serious post-operative complications have been reported including intraocular pressure elevation, retinal detachment, cystoid macular edema, lens pitting and IOL damage [15–20]. Thus, novel non-toxic pharmacological approaches to prevent PCO formation are of high clinical interest.

In the case of PCO, using the IOL as a drug delivery system bears several potential advantages. These are, for example, the direct vicinity of the IOL to the PCO cells on the posterior capsule, which allows a drug release to directly reach the target. Low concentrations of drug in the IOL might therefore be effective while being less toxic to the numerous surrounding tissues in the anterior segment of the eye. Implanting a topic drug delivery device during surgery reduces the risk of lacking patient compliance as the need for eyedrops is alleviated. It is also comfortable for the surgeon as surgical time is not extended since no additional steps are required.

In this context, IOLs were either loaded or coated with various active pharmaceutical ingredients to prevent PCO. Hydrophilic acrylic (hydrogels) IOLs were impregnated using the soaking in liquid method by immersing IOLs in distilled water solutions of tranilast (1 $mg.mL^{-1}$), diclofenac sodium (0.2 $mg.mL^{-1}$), mitomicin C (0.2 $mg.mL^{-1}$), colchicine (12.5 $mg.mL^{-1}$) and 5-fluorouracile (10 $mg.mL^{-1}$) under sterile conditions at 37 °C for 3 hours. Tranilast, diclofenac sodium and 5-fluorouracil coated IOLs were shown to inhibit the adhesion and growth of epithelial cells on lenses, thus allowing PCO prevention [21]. Silicone IOLs were soaked in a 50% ethanol-50% water sterile solution containing dexamethasone (1 $mg.mL^{-1}$) for 40 minutes and were then washed with sterile water and air-dried [22]. Erufosin was loaded into foldable hydrophobic, hydrophilic or hydrophilic with hydrophobic surface IOLs by a liquid impregnation method [23,24]. Liu *et al.* [25] prepared rapamycin delivery systems by surface modification of PMMA IOLs achieved by spraying a 1% (w/w) solution of PLGA (50/50; MW, 12000) in chloroform containing an appropriate amount of rapamycin, onto the edge of IOL optics. Kassumeh *et al.* [26] spray-coated methotrexate-loaded PLGA microspheres both on hydrophilic and hydrophobic acrylic IOLs. All the systems showed good laboratory scale results supported by experimental *in vivo* and *ex vivo* settings, but to our knowledge have not yet made their way through translation research into clinics.

One of the reasons for this lies in the fact that conventional impregnation methods, as well as dip and spray-coating methods, are reliant on organic solvents to allow solubilization of most lipophilic drugs. Several drawbacks are inherent to the use of organic solvents such as their

well-described toxicity which will be exerted by the presence of residual traces in the final implant. In addition, their reactivity might lead to undesired chemical reactions with the pharmacological agent, the IOL polymer or the carrier molecule. Photochemical or thermal degradation of any part of the modified IOL might also be enhanced or altered by the presence of solvents. Furthermore, low loading yields**,** heterogeneous drug incorporation/dispersion**,** limited depth of penetration**,** low diffusion rates, long contact durations [27–29] are often observed.

To overcome these issues, the supercritical impregnation technology was selected in the present work, using the generally recognized as safe (GRAS) supercritical carbon dioxide ($scCO_2$) as the impregnation carrier. The specific properties of supercritical fluids (high density, low viscosity, diffusivity higher than that of liquids, low interfacial tension, etc.) make them good candidates for impregnation. For medical and pharmaceutical processing, $scCO_2$ has the advantage of mild critical conditions especially in terms of temperature (Pc = 7.38 MPa and Tc = 31.06 °C). Moreover, under ambient pressure and temperature conditions, CO_2 is gaseous and therefore its separation at the end of the process is spontaneous upon depressurization. Besides, $scCO_2$ has biocidal properties [30], which provide further advantages for medical applications.

Supercritical impregnation of intraocular and contact lenses has successfully proven its applicability in developing topical sustained drug release delivery systems [27,28,31–39]. Furthermore, when compared to conventional soaking methods, supercritical impregnation is more efficient and adjustable while requiring shorter processing durations [28,40].

Our previous work featured the potential of the supercritical impregnation process to develop sustained release drug delivery IOLs for the prevention of endophthalmitis, a rare but devastating postoperative complication of cataract surgery [33,36–38]. Polymer IOLs from different natures were used as drug support: rigid hydrophobic (derivative from PolyMethyl Methacrylate, [PMMA]), foldable hydrophobic (blends of PMMA and poly-2-hydroxyethyl methacrylate [P-HEMA]) as well as foldable hydrated (derivative from P-HEMA) IOLs. Furthermore, several drug components were loaded in the aforementioned IOLs: cefuroxime sodium and ciprofloxacin (antibiotics) and dexamethasone 21-phosphate disodium (an anti-inflammatory drug). Transparency of the impregnated IOLs were shown to be maintained by respecting controlled pressurization and depressurization rates, thus avoiding the occurrence of undesirable foaming phenomena [36,37]. In these conditions, the characterization of the optical properties according to the standards stated by the International Organization for Standardization (ISO 11979-2:2014) has shown that the dioptric power, as well as the imaging quality, were fulfilled [38]. For all the investigated drug/IOL systems, *in vitro* drug release studies indicated a sustained release for durations ranging from a few days to a few tens of days without a burst effect indicating an effective and in-depth impregnation. The drug loadings as well as the drug release profiles and durations varied according to the chemical structure of the drug and IOL compounds but also on the experimental conditions. These studies highlighted the difficulty to predict drug loading when varying the investigated polymer IOL and drug component as several concomitant interaction phenomena are involved in the process: the sorption of $scCO_2$ in the polymer support, the polymer swelling as well as the solubilization of the drug in supercritical CO_2 and its partitioning between the polymer and the fluid phase

according to relative affinities. All these interactions can be influenced by varying the operating conditions of pressure, temperature and impregnation duration as well as by the addition of a co-solvent.

The purpose of this study was to develop innovative sustained release drug delivery IOLs for PCO prevention using supercritical impregnation. Our previous works revealed that, in a systematic *in vitro* evaluation of 62 pharmacological substances in human lens epithelial cells and human capsular bags, methotrexate was suitable for the prevention of PCO at very low concentrations (nanomolar), while being non-toxic to cells of the surrounding tissues [26,41]. As an antimetabolite for folic acid synthesis, it was shown to be able to attenuate the major cellular features associated with PCO formation (lens epithelial cell proliferation, migration, and contraction) and was therefore selected to be loaded into commercially available foldable hydrophobic acrylic IOLs. Available, approved and in clinical use for more than 60 years, methotrexate is well-characterized in human treatment and is in off-lable clinical use by intravitreal injection. Therefore, methotrexate is a good candidate for impregnation studies.

As far as we know, no literature work reports the application of the supercritical impregnation process to methotrexate. Only particle generation processes using supercritical CO_2 as an anti-solvent were applied either to micronize methotrexate through the Solution-Enhanced Dispersion by Supercritical fluids (SEDS) process [42] or to coprecipitate/encapsulate methotrexate with polymeric supports by forming methotrexate-PLLA–PEG–PLLA or methotrexate-Fe_3O_4–PLLA–PEG–PLLA composite microspheres using the Suspension-Enhanced Dispersion by Supercritical CO_2 (SpEDS) process [43,44]. In this study, supercritical impregnation process was applied to load methotrexate within polymer intraocular lenses. The influence of operating conditions of supercritical impregnation (pressure and duration) on *in vitro* drug release as well as on drug loading was studied either when using pure supercritical CO_2 as drug carrier or when adding ethanol as a co-solvent (polar modifier). After having implemented a suitable supercritical impregnation method, the originality of this study was to evaluate *ex vivo* the effect of loaded IOLs on human lens epithelial cell proliferation using a human capsular bag model. Furthermore, in order to determine whether the level of fibrosis is influenced by methotrexate loading into IOLs, immunofluorescence staining of three common fibrosis markers, fibronectin, f-actin and α-smooth muscle actin was carried out.

2 Materials and methods

2.1 Materials

Commercially foldable hydrophobic acrylic (acrylate-methacrylate copolymers) IOLs were used (UF60125, Bausch&Lomb, Rochester, NY, USA). Methotrexate ($C_{20}H_{22}N_8O_5$, 454.44 $g.mol^{-1}$) (Millipore/Sigma, France) was stored at -20°C (Fig. 1). Carbon dioxide (99.7% purity) (Air Liquide, France) was used as the supercritical fluid and ethanol (≥ 99.8% purity) (Groupe MERIDIS, Montpellier, France) as a polar modifier.

2.2 Supercritical impregnation

Supercritical impregnations were carried out in a batch mode because of its simplicity to handle. A moderate temperature of 308 K was set thus allowing to be in supercritical conditions while

avoiding any thermal degradation of drug components. The influence of the operating conditions on methotrexate impregnation into IOLs was studied by varying the pressure (8 and 25 MPa) and the duration (30 and 240 min), either while using pure supercritical CO_2 as impregnation carrier or when adding a co-solvent (5 mol% ethanol) to the supercritical fluid phase. Ethanol, a solvent miscible in all proportions with $scCO_2$ was selected as a polar modifier in order to enhance drug solubility in the $scCO_2$ and polymer swelling [45] . It is also a 'class 3' solvent according to the FDA which is considered as safe for human health [46].

The experimental set-up and protocol were previously described [36–38]. The set-up is illustrated in Fig. 2 and is mainly composed of a 125 mL high-pressure cell (Top Industrie S.A., Vaux-le-Pénil, France) immersed in a temperature-controlled bath and placed on a magnetic stirrer. In an experimental batch, each IOL was protected by a frit filter and placed on an aluminum support within the high-pressure cell to avoid any contact with the magnetic stirring bar. 5 mg of drug were also introduced in a frit filter and deposited on the aluminium support. When ethanol is used as co-solvent, a predefined quantity was firstly loaded at the bottom of the autoclave. After heating the high-pressure cell, it was supplied with preheated CO_2 until reaching the desired pressure. A predefined impregnation duration was respected to allow drug dissolution and fluid phase diffusion within the IOLs at constant pressure and temperature, before depressurization to atmospheric pressure. For impregnations carried out using a co-solvent, a washing step was carried out before depressurization in order to remove ethanol from the high-pressure cell. For that purpose, pure $scCO_2$ was flowed into the impregnation vessel for 5 times the residence time considering that the autoclave behaves like a stirred tank reactor [47].

For all the impregnations, a constant pressurization flow rate of 250 $g.h^{-1}$ and a depressurization rate of 0.2 $MPa.min^{-1}$ were found to prevent unintended IOL foaming [33,36,37].

For the *ex vivo* human capsular bag assays, control IOLs with equal supercritical treatment under the same experimental conditions, but without methotrexate, were used to exclude confounding factors.

2.3 Drug release study

In vitro drug release studies were conducted on methotrexate loaded IOLs. For this purpose, the impregnated IOLs were suspended in 3 mL of a simulated aqueous humor (pH of 7.2), prepared as described by Masmoudi et al. [33], at 37°C and under constant stirring. Aliquots of 0.4 mL were collected regularly, and drug concentration was quantified at 260.4 nm using a spectrophotometer (Jenway 6715 UV/VIS, Stafordshire, UK) and following the calibration curve (Eq. (1) established with a coefficient of determination of 0.997) relating the concentration of methotrexate in the simulated aqueous humor (C_{MTX} expressed in $\mu g.mL^{-1}$) to the absorbance (A).

$$C_{MTX}=20.76\ A \qquad \text{Eq. (1)}$$

After each analysis, the aliquot was returned to the release vessel to maintain the initial volume. The drug loading (DL) was calculated according to the following equation:

$$DL = \frac{m_{imp}}{m_{0IOL}} \quad \text{Eq. (2)}$$

where m_{0IOL} is the mass of the non-processed IOL and m_{imp} is the mass of impregnated drug corresponding to the mean accumulated drug released after reaching a plateau.

The release duration ($t_{release}$) corresponds to the time at which m_{imp} is reached.

The experimental drug release curves were fitted using the Korsmeyer-Pepas (empirical) model (Eq. (3() [48,49]. This equation is only valid to analyze the drug release profile below 60% of the whole accumulated mass released from non-swellable polymeric delivery systems.

$$\frac{m_t}{m_{imp}} = k\, t^n \quad \text{Eq. (3)}$$

where m_t and m_{imp} are the absolute cumulative amounts of released drug at time t and at infinite release time, respectively. k is a kinetic constant incorporating the structural and geometric characteristics of a delivery system and n is designated as an exponent representing the release mechanism. For a thin film, the drug release mechanisms can be distinguished as a pure Fickian diffusional behavior when n is equal to 0.5, a swelling-controlled release if n is equal to 1 and an anomalous (non Fickian) release coupling diffusion and swelling phenomena when n is between 0.5 and 1 [49]. To identify k and n values, $\ln(m_t/m_{imp})$ was plotted versus ln(t). The slope of the trendline is n and ln(k) is the y-intercep t. The value of the coefficient of determination (r^2) indicates the quality of the linear regression.

2.4 Human capsular bag preparation

The human capsular bags were prepared as described by Cleary *et al.* [50], with certain modifications. In brief, 6 cadaver eyes from 3 human donors, not available for transplantation purposes, were obtained from the Institute of Forensic Medicine, Ludwig-Maximilians-University Munich, (Germany) and processed within 4 to 24 hours of death. None of the donors had a known history of eye disease. Methods for securing human tissue were humane, included proper consent and approval, complied with the Declaration of Helsinki and were approved by the local ethics committee (Approval ID: 73416). Corneoscleral discs had already been removed for transplantation purposes. Methotrexate loaded IOLs and control IOLs were implanted into the capsular bags by open-sky cataract surgery. In order to preserve normal capsular and zonular architecture, the IOL-capsule-zonule-ciliary-body complex was dissected from the globe in one piece and stretched out on a soft silicone ring by piercing thin entomological pins through the ciliary body and the silicone ring. The capsule was supported by the native zonules and suspended freely within culture medium.

2.5 Cell Culture

Specimens were cultured on cell culture plates (NUNC, Langenselbold, Germany). The culture

medium (MEM Earls, Biochrom AG, Berlin, Germany) was supplemented with 2% fetal calf serum (Biochrom AG, Berlin, Germany), 50 IU penicillin/mL, 50 µg streptomycin/mL (Biochrom AG, Berlin, Germany). Tissue was kept under standard cell culture conditions in an incubator at 37 °C and an atmosphere enriched with 5% carbon dioxide. The culture medium was replaced every second day. A microscopic photograph was taken daily. The IOL-optic-area free of PCO cells was measured on the photographs using ImageJ 1.8.0 (NIH, Bethesda, MD, USA).

2.6 Immunofluorescence staining

Immunofluorescence staining was performed on all specimens. After cultivation in tissue culture, the capsular bags were washed three times with phosphate-buffered saline (PBS Dulbecco, L1825, Biochrom AG, Berlin, Germany) before being fixed in a 4% solution of paraformaldehyde (Sigma-Aldrich, St. Louis, MO, USA) in distilled water overnight. Three additional washing steps in 0.1 M phosphate buffer ((Na_2HPO_4 x $2H_2O$ + NaH_2PO_4 x H2O 1:1; Merck, Darmstadt, Germany) in distilled water were performed. The IOL was then carefully extracted, and the zonules were cut under the microscope to free the capsular bag. The posterior capsule was divided into quarters and fixed again with entomological pins to a cell culture well and incubated with blocking solution (3% bovine serum albumin fraction V (Roche Diagnostics, Mannheim, Germany) and 0.1% Triton X 100 (Carl Roth, Karlsruhe, Germany) in 0.1 M phosphate buffer) to block unspecific antigen staining and for antigen unmasking.

F-Actin was stained without antibody by Alexa fluor 488 conjugated phalloidin (A12379, Invitrogen, Carlsbad, CA, USA) for 120 min. A directly cyanine dye (Cy3) conjugated antibody purified from hybridoma cell culture (C6198 Sigma-Aldrich, St. Louis, Missouri, USA) was used for α-smooth muscle actin in a dilution of 1:50. Primary rabbit antibodies were used for fibronectin (F3648, Sigma-Aldrich, St. Louis, Missouri, USA) and collagen 1 (ab34710, Abcam, Cambridge, UK) in a dilution of 1:50. The specimens were labelled overnight at 4 °C with either one of the primary antibodies. Another washing step preceded the incubation with the secondary antibodies for 60 min. A Goat anti-Rabbit Alexa fluor 555 (A27039, Invitrogen, Carlsbad, CA, USA) served as a secondary antibody in a dilution of 1 : 500 for 120 min at room temperature for fibronectin.

After antibody labelling and washing three times with 0.1 M phosphate buffer, the nuclei were stained using Hoechst 33342 (Invitrogen, Carlsbad, CA, USA) in a dilution of 1 : 2000 in 0.1 M phosphate buffer. After three washing steps in 0.1 M phosphate buffer, the capsular bag was then mounted in en face flat mount technique onto glass slides and conserved with vectashield antifade mounting for fluorescence medium (Vector Laboratories, Burlingame, CA, USA). Marked epitopes were examined with an inverse microscope with a digital camera (Axio Observer 3, Carl Zeiss AG, Jena, Germany) and the ZEN software (Carl Zeiss AG, Jena, Germany).

2.7 Experimental error calculations and statistical analysis

For all the experimental release studies, each concentration point was measured in triplicate. The maximum absolute error of total released mass m_{imp} was set to be ± 0.5 µg, as this was the highest experimental fluctuation in the accumulated released mass when the plateau was reached. This value was then used to estimate the error in the impregnation release duration ($t_{release}$), by the determination of the maxium deviation of $t_{release}$ that corresponded to the maximum absolute error of m_{imp} (± 0.5 µg). Using this method, the maximum deviation of $t_{release}$ was set to be ± 7 days. Supercritical impregnation repeatability was also tested in 3 preliminary sample repeats using pure $scCO_2$ (without co-solvent) at 25 MPa and 308 K for 240 min, using IOLs with a diopter power of +23.0 D.

Statistical comparison between experimental groups in the human capsular bag model was carried out using an ANOVA with an LSD post-hoc test. For all analyses, $p<0.05$ was considered statistically significant. All graphs were plotted in Prism 8 (GraphPad Software, CA, USA) or by Excel 365 (Microsoft, Albuquerque, NM, USA) with the mean displayed and the standard deviation as an error bar. All statistical analyses were performed by SPSS 24.0 (IBM, Armonk, NY, USA) and all calculations were carried out by Excel 365.

3 Results

3.1 Supercritical impregnation of methotrexate in intraocular lenses

As aforementioned, 3 preliminary impregnations of IOLs (+23.0 D) were repeated using pure $scCO_2$ (without co-solvent) at 25 MPa and 308 K for 240 min. The drug released mass was measured twice a week until reaching a constant value. The average methotrexate impregnated mass per IOL (m_{imp} = 8.1 ± 0.4 µg) and drug loading (DL = 0.44 ± 0.02 $\mu g.mg^{-1}_{IOL}$) laid within the experimental error range (respectively 0.5 µg and 0.03 $\mu g.mg^{-1}_{IOL}$) therefore showed good repeatability (Table 1).

After having shown the repeatability at high pressures, the influence of a lower pressure (8 MPa vs. 25 MPa) and lower duration (30 vs. 240 min) on impregnation was studied at 308 K either with pure supercritical CO_2 or after the addition of a co-solvent (5 mol% ethanol) using 6 IOLs (+20.0 D). Drug loadings (DL) varying between 0.43 to 0.75 ± 0.03 $\mu g_{drug}.mg^{-1}_{IOL}$ were obtained. The drug release was complete after a $t_{release}$ varying from 87 to 117 ± 7 days (Table 2 and Fig. 3). The drug loading obtained in similar conditions than the repeatability tests but with an IOL diopter power of +20.0D was of 0.43 $\mu g_{drug}.mg^{-1}_{IOL}$ which is coherent with the repeatability loading (0.44±0.02).

3.2 Human capsular bag model

Three pairs of eyes were implanted with IOLs either loaded with methotrexate at 25 MPa and 308 K during 240 min or with control IOLs that received similar supercritical treatment without the addition of methotrexate. For each pair (implanted with loaded /control IOLs), the evolution of the IOL area free of PCO cells until full coverage is compared in Fig. 4. The cell in the experimental group without IOL implantation fully covered the region of the optical axis after a mean of 11.6 ± 1.5 days. The implantation of a methotrexate IOL could increase this time by about two-fold to 22.8 ± 10.6 days (p=0.1). The difference between the two IOLs was not

statistically significant.

After cultivation, the cells on the central posterior capsule, which were located below the IOL, were evaluated by immunofluorescence staining as this is the relevant pathological area for PCO. Fig. 5 compares specific immunofluorescence images for fibronectin, F-actin and α-SMA on both control and methotrexate loaded IOLs. Cells on the posterior capsule of capsular bags with an implanted IOL showed specific immunostaining for fibronectin, F-actin and α-SMA. Fibronectin is normally secreted by the cells to the extracellular matrix to initiate adhesion. Fibronectin was equally distributed in the control group and in the methotrexate modified IOLs. The localization was adjacent to the cytoplasmatic part of the cells.

The cell morphology in the methotrexate modified IOL was mainly epithelial, whereas the control indicated a more fibroblastic phenotype. These findings were underlined by the reduced expression of α-SMA in the methotrexate modified IOLs and coincided with the typical distribution pattern of F-actin. The actin cytoskeleton in the methotrexate modified IOL was mainly distributed in a circular pattern in the periphery of the cytoplasm, which is consistent with an epithelial phenotype, whereas the control showed a diffuse linear actin distribution, indicating greater consistence with a fibroblastic phenotype (Fig. 5).

4 Discussion

Preliminary experiments, performed on IOL (diopter +23.0D) at 25 MPa, 308 K and for a duration of 240 min, were proven to be repeatable in triplicate leading to a satisfactory drug loading and variation of 0.44 ± 0.03 $\mu g.mg^{-1}_{IOL}$ corresponding to an average methotrexate impregnated mass per IOL of 8.1 ± 0.5µg. After validating the experimental repeatability, the drug delivery through the IOLs was studied at 308 K under different experimental conditions of pressure and duration (Table 2). This was done to explore the possibility of milder impregnation conditions in order to lower the risk of damaging the implant, which is highly reliant on its shape, flexibility, radial curvature and flexibility for its clinical purpose. Sustained release for a long duration ranging between 87 and 117 days was achieved without a burst effect, indicating an in-depth impregnation (Fig. 3). The methotrexate concentration, that was eluted from the IOL did have a biological effect against cellular responses normally seen in PCO *in vitro* [51]. The drug loadings ranged between 0.43 and 0.75 $\mu g_{drug}.mg^{-1}_{IOL}$. The highest total mass of impregnated methotrexate was obtained for IOLs loaded at 8 MPa and 308 K for 240 min without using a co-solvent. All the release exponent values (n) are close to 0.5 with a coefficient of determination above 0.91, indicating a Fickian diffusion release mechanism.

In the absence of a co-solvent, higher drug loadings were obtained when impregnation duration was extended from 30 to 240 min. This result can be explained by a higher concentration of methotrexate in $scCO_2$ at longer duration in the case in which the time required to reach thermodynamic equilibrium of methotrexate dissolution is longer. Furthermore, a longer impregnation duration favors $scCO_2$ sorption throughout the polymer, possibly as $scCO_2$ sorption requires a certain duration to do so, depending on the operating conditions, the chemical nature and the geometric characteristics of the polymeric matrix [38]. Consequently, the relaxation of the polymer and the swelling, assisting the fluid phase penetration within the polymeric IOLs, can be enhanced at longer durations. Comparable findings were described in

literature regarding the impregnating of commercially available contact lenses with ophthalmic drugs [36,40], indicating that a slightly longer release time was observed for longer impregnations, corresponding to a more in-depth loading.

For a similar long impregnation duration of 240 min, increasing the pressure from 8 to 25 MPa, leads to a 43% reduction of the drug loading (from 0.75 to 0.43 ± 0.03 $\mu g.mg^{-1}_{IOL}$) and a decrease in the release time (from 117 to 87 ± days). Even if to our knowledge no data on methotrexate solubility in $scCO_2$ are reported in literature, since $scCO_2$ density increases at higher pressures, thus enhancing methotrexate solubility in $scCO_2$, the solute partition could become more favorable towards the supercritical phase**.** Furthermore, at higher $scCO_2$ densities, the fluid phase sorption within polymers can be enhanced favoring the corresponding polymer swelling, which may facilitate the solute drag out from a more swollen polymeric matrix during depressurization. In literature, even if an increase in pressure results predominantly in favoring impregnation, some authors report similar findings as obtained in this work [37,46,52–54]. The effect is often explained on the basis of $scCO_2$/drug interactions that prevail over the polymer/drug interactions.

In this study, when ethanol, a co-solvent used for many medical applications, was added to the fluid phase to increase its polarity, no significant influence on drug loading nor on release time was observed. The close results could be explained by a higher solubility of methotrexate in the fluid phase which could be counterbalanced by lower sorption of ethanol/$scCO_2$ the in hydrophobic polymer. As the addition of ethanol as a co-solvent did not improve impregnation, its use can be dispensed, which is preferred for medical devices that are applied to the sensitive intraocular environment.

After cataract surgery, the lens epithelial cells attached to the anterior and equatorial capsular bag can proliferate and spread to the center of the visual axis between the IOL surface and the posterior capsule. Previously, methotrexate was shown to counteract this effect [26,41]. In the cell culture of an immortalized lens epithelial cell line (FHL-124), the efficient concentration (EC_{50}) for blocking cell proliferation of those cells was found to be of 98 nM in the medium [41]. The total amount of methotrexate incorporated into the IOL in this study varied between 8.4 and 13.5 µg and therefore between 18.5 and 29.7 nmol of drug. If this amount of drug were to be released instantly to the 3 mL cell culture medium used in this study, a total concentration of about 6.2 to 9.9 µM would be achieved. As shown above, the release does happen over a period of about 100 days and, as a standard, the medium was replaced every second day. Therefore, conservatively the maximum molar concentration of methotrexate at the end of the two days in the medium reached around 123 to 198 nM. In accordance with our previous works and even though another model was used, a biological effect of methotrexate can be expected and was confirmed above [41]. It is worth noting that the concentration at the lens epithelium could be even higher due to the direct contact of the IOL to the PCO cells on the posterior capsule. Further studies are required to deteremine whether the drug concentrations are useable for a clinical application especially in the light of the very complex turnover and volume of aqueous humor and vitreous body in the complicate pharmacologic compartment of the eyeball.

Epithelial to mesenchymal transformation of lens epithelial cells is the origin of myofibroblastic transdifferentiated cells which are a major factor in PCO formation [55]. The process of

transdifferentiation is activated by several growth factors and cytokines and leads to the expression of certain proteins and cellular behavior, which are not present in the healthy lens epithelium. α-SMA is one of the proteins involved in the fibrotic response, which causes contraction of cells and is strongly implicated in PCO formation [3]. As a result, clinically a decrease in vision, capsule wrinkling, fibrosis, phimosis or IOL dislocation could be clinically observed [56]. In our experiments, we detect a higher amount of α-SMA positive cells in the controls. Hence, the release of methotrexate from the loaded IOLs seems to block the formation of epithelial-mesenchymal transition of cells at the posterior lens capsule indicating a positive biological effect of the application described. In addition, the F-actin cytoskeleton in the methotrexate modified IOL was mainly distributed in a circular pattern in the periphery of the cytoplasm, which is consistent with an epithelial phenotype. Myofibroblasts furthermore overexpress fibronectin, which allows them to bind to extracellular matrix. Fibronectin modulates and stabilizes the extracellular matrix in wound healing processes [57]. Fibronectin was present in the expected location extracellularly and enhanced below the IOLs and in the capsular folds, where increased fibrotic cell activity is suspected.

As an FDA and EMA approved substance for many different disease entities, methotrexate is used and extensively characterized in the clinical and pre-clinical setting since the 1950s. In ophthalmology, the drug serves as an off-label intravitreal injection for lymphoma [58]. Clinical studies have also been reported on an intravitreal slow release device for treatment of chorioiditis [59]. One group has employed methotrexate for the treatment of diabetic macular edema in humans and found that, after a 6-month follow-up study, intravitreal injection of 400 µg has no significant effect on corneal endothelial cells [60]. These data are very promising for the safety of our application, but of course, further studies are needed to determine the toxicity of methotrexate when released into the anterior segment by a supercritical fluid impregnated IOL.

5 Conclusions

In order to mitigate PCO, supercritical impregnation of methotrexate, an antimetabolite drug for folate acid production, into IOLs used in cataract surgery was carried out in order to allow a sustained drug delivery from the implant. Supercritical impregnation conditions of pressure (8 and 25 MPa) and duration (30 and 240 min) were varied at 308 K leading to drug loadings ranging between 0.43 to 0.75 $\mu g_{drug}.mg^{-1}_{IOL}$ with a sustained release for more than 80 days. Even for the most lightly loaded IOLs (0.43 $\mu g_{drug}.mg^{-1}_{IOL}$ for IOLs impregnated with pure CO_2 at 25 MPa and 308 K for 240 min), the drug loading was high enough to produce a biological effect of the IOLs *in vitro* in the human capsular bag model stated by a reduced expression of α-SMA withthe methotrexate modified IOLs and coincided with the typical distribution pattern of F-actin. Further studies are needed to evaluate the clinical potential of the described application.

Acknowledgment

The authors would like to thank the Thai Ministry of Science and Technology for providing the Royal Thai Government Scholarship to support the PhD thesis of Kanjana Ongkasin.

References

[1] W.R. Meacock, D.J. Spalton, J. Boyce, J. Marshall, The Effect of Posterior Capsule Opacification on Visual Function, Investig. Opthalmology Vis. Sci. 44 (2003) 4665. https://doi.org/10.1167/iovs.02-0634.

[2] I.M. Wormstone, L. Wang, C.S.C. Liu, Posterior capsule opacification, Exp. Eye Res. 88 (2009) 257–269. https://doi.org/10.1016/j.exer.2008.10.016.

[3] D.Y. Shu, F.J. Lovicu, Myofibroblast transdifferentiation: The dark force in ocular wound healing and fibrosis, Prog. Retin. Eye Res. 60 (2017) 44–65. https://doi.org/10.1016/j.preteyeres.2017.08.001.

[4] T. Mosmann, Rapid colorimetric assay for cellular growth and survival: application to proliferation and cytotoxicity assays, J. Immunol. Methods. 65 (1983) 55–63. https://doi.org/10.1016/0022-1759(83)90303-4.

[5] M.C.J. van Bree, I.J.E. van der Meulen, L. Franssen, J.E. Coppens, N.J. Reus, B.L.M. Zijlmans, T.J.T.P. van den Berg, Imaging of Forward Light-Scatter by Opacified Posterior Capsules Isolated from Pseudophakic Donor Eyes, Investig. Opthalmology Vis. Sci. 52 (2011) 5587. https://doi.org/10.1167/iovs.10-7073.

[6] H.C. Chen, C.Y. Lee, C.C. Sun, J.Y. Huang, H.Y. Lin, S.F. Yang, Risk factors for the occurrence of visual-threatening posterior capsule opacification, J. Transl. Med. 17 (2019) 209. https://doi.org/10.1186/s12967-019-1956-6.

[7] J.C. Erie, M.E. Raecker, K.H. Baratz, C.D. Schleck, D.M. Robertson, Risk of retinal detachment after cataract extraction, 1980-2004: a population-based study, Trans. Am. Ophthalmol. Soc. 104 (2006) 167–175. https://doi.org/10.1016/j.ophtha.2006.05.054.

[8] J.W. Cheng, R.L. Wei, J.P. Cai, G.L. Xi, H. Zhu, Y. Li, X.Y. Ma, Efficacy of Different Intraocular Lens Materials and Optic Edge Designs in Preventing Posterior Capsular Opacification: A Meta-Analysis, Am. J. Ophthalmol. 143 (2007) 428-436.e3. https://doi.org/10.1016/j.ajo.2006.11.045.

[9] P.G. Ursell, M. Dhariwal, D. O'Boyle, J. Khan, A. Venerus, 5 year incidence of YAG capsulotomy and PCO after cataract surgery with single-piece monofocal intraocular lenses: a real-world evidence study of 20,763 eyes, Eye. (2019). https://doi.org/10.1038/s41433-019-0630-9.

[10] C.M. Bell, W.V. Hatch, G. Cernat, D.R. Urbach, Surgeon Volumes and Selected Patient Outcomes in Cataract Surgery, Ophthalmology. 114 (2007) 405–410. https://doi.org/10.1016/j.ophtha.2006.08.036.

[11] S. Sacu, R. Menapace, W. Buehl, G. Rainer, O. Findl, Effect of intraocular lens optic edge design and material on fibrotic capsule opacification and capsulorhexis contraction, J. Cataract Refract. Surg. 30 (2004) 1875–1882. https://doi.org/10.1016/j.jcrs.2004.01.042.

[12] D.J. Apple, Q. Peng, N. Visessook, L. Werner, S.K. Pandey, M. Escobar-Gomez, J. Ram, G.U. Auffarth, Eradication of posterior capsule opacification: documentation of a marked decrease in Nd:YAG laser posterior capsulotomy rates noted in an analysis of 5416 pseudophakic human eyes obtained postmortem, Ophthalmology. 108 (2001) 505–518. https://doi.org/10.1016/s0161-6420(00)00589-3.

[13] L. Vock, R. Menapace, E. Stifter, M. Georgopoulos, S. Sacu, W. Bühl, Posterior capsule opacification and neodymium:YAG laser capsulotomy rates with a round-edged silicone and a sharp-edged hydrophobic acrylic intraocular lens 10 years after surgery, J. Cataract Refract. Surg. 35 (2009) 459–465. https://doi.org/10.1016/j.jcrs.2008.11.044.

[14] P. Sahu, A.K. Mishra, Safety and efficacy of Nd:YAG laser capsulotomy in management of posterior capsular opacification, Int. J. Adv. Med. 6 (2019) 76. https://doi.org/10.18203/2349-3933.ijam20190108.

[15] Does Nd:YAG Capsulotomy Increase the Risk of Retinal Detachment?, Asia-Pac. J. Ophthalmol. (2018). https://doi.org/10.22608/APO.2018275.

[16] H. Elzarrug, K.M. Miller, Y. Fei, A.E.M. Daifalla, Risk Factors for Postoperative Retinal Detachment Following Cataract Surgery, Open J. Ophthalmol. 09 (2019) 141–150. https://doi.org/10.4236/ojoph.2019.93015.

[17] J.C. Javitt, J.M. Tielsch, J.K. Canner, M.M. Kolb, A. Sommer, E.P. Steinberg, National outcomes of cataract extraction. Increased risk of retinal complications associated with Nd:YAG laser capsulotomy. The Cataract Patient Outcomes Research Team, Ophthalmology. 99 (1992) 1487–1497; discussion 1497-1498. https://doi.org/10.1016/s0161-6420(92)31775-0.

[18] T.J. Newland, G.U. Auffarth, T.A. Wesendahl, D.J. Apple, Neodymium:YAG laser damage on silicone intraocular lenses. A comparison of lesions on explanted lenses and experimentally produced lesions, J. Cataract Refract. Surg. 20 (1994) 527–533. https://doi.org/10.1016/s0886-3350(13)80233-7.

[19] M. Mangane, V. Reddy, R. Reddy, Effect of Nd:YAG laser in the management of posterior capsulotomy after extracapsular cataract extraction, Int. J. Med. Sci. Public Health. 7 (2017) 1. https://doi.org/10.5455/ijmsph.2018.1029408112017.

[20] A. Parajuli, P. Joshi, P. Subedi, C. Pradhan, Effect of Nd:YAG laser posterior capsulotomy on intraocular pressure, refraction, anterior chamber depth, and macular thickness, Clin. Ophthalmol. Volume 13 (2019) 945–952. https://doi.org/10.2147/OPTH.S203677.

[21] H. Matsushima, K. Mukai, N. Gotoo, S. Yoshida, T. Yoshida, M. Sawano, T. Senoo, Y. Obara, J.I. Clark, The effects of drug delivery via hydrophilic acrylic (hydrogel) intraocular lens systems on the epithelial cells in culture, Ophthalmic Surg. Lasers Imaging Off. J. Int. Soc. Imaging Eye. 36 (2005) 386–392. https://doi.org/10.3928/1542-8877-20050901-07.

[22] M. Kugelberg, K. Shafiei, I. van der Ploeg, C. Zetterström, Intraocular lens as a drug delivery system for dexamethasone, Acta Ophthalmol. (Copenh.). 88 (2010) 241–244. https://doi.org/10.1111/j.1755-3768.2008.01419.x.

[23] K.H. Eibl, C. Wertheimer, M. Kernt, A. Wolf, D. Kook, C. Haritoglou, A. Kampik, Alkylphosphocholines for intraocular lens coating, J. Cataract Refract. Surg. 39 (2013) 438–445. https://doi.org/10.1016/j.jcrs.2012.09.028.

[24] L.R. Wertheimer C, W.A. Kampik A, E. Lindner KH, Erufosine Coated Hydrophilic Intraocular Lenses Attenuate PCO Formation in Vitro, J. Clin. Exp. Ophthalmol. 06 (2015). https://doi.org/10.4172/2155-9570.1000453.

[25] H. Liu, L. Wu, S. Fu, Y. Hou, P. Liu, H. Cui, J. Liu, L. Xing, X. Zhang, Polylactide-glycoli acid and rapamycin coating intraocular lens prevent posterior capsular opacification in rabbit eyes, Graefes Arch. Clin. Exp. Ophthalmol. 247 (2009) 801–807. https://doi.org/10.1007/s00417-008-1007-0.

[26] S.A. Kassumeh, C.M. Wertheimer, A. von Studnitz, A. Hillenmayer, C. Priglinger, A. Wolf, W.J. Mayer, D. Teupser, L.M. Holdt, S.G. Priglinger, K.H. Eibl-Lindner, Poly(lactic-co-glycolic) Acid as a Slow-Release Drug-Carrying Matrix for Methotrexate Coated onto Intraocular Lenses to Conquer Posterior Capsule Opacification, Curr. Eye Res. 43 (2018) 702–708. https://doi.org/10.1080/02713683.2018.1437455.

[27] M.E.M. Braga, M.T.V. Pato, H.S.R.C. Silva, E.I. Ferreira, M.H. Gil, C.M.M. Duarte, H.C. de Sousa, Supercritical solvent impregnation of ophthalmic drugs on chitosan derivatives, J. Supercrit. Fluids. 44 (2008) 245–257. https://doi.org/10.1016/j.supflu.2007.10.002.

[28] C. González Chomón, M.E.M. Braga, H.C. de Sousa, A. Concheiro, C. Alvarez-Lorenzo, Antifouling foldable acrylic IOLs loaded with norfloxacin by aqueous soaking and by supercritical carbon dioxide technology, Eur. J. Pharm. Biopharm. 82 (2012) 383–391. https://doi.org/10.1016/j.ejpb.2012.07.007.

[29] E. Weidner, Impregnation via supercritical CO2–What we know and what we need to know, J. Supercrit. Fluids. 134 (2018) 220–227. https://doi.org/10.1016/j.supflu.2017.12.024.

[30] M. Perrut, Sterilization and virus inactivation by supercritical fluids (a review), J. Supercrit. Fluids. 66 (2012) 359–371. https://doi.org/10.1016/j.supflu.2011.07.007.

[31] A.R.C. Duarte, A.L. Simplicio, A. Vega-González, P. Subra-Paternault, P. Coimbra, M.H. Gil, H.C. de Sousa, C.M.M. Duarte, Impregnation of an intraocular lens for ophthalmic drug delivery, Curr. Drug Deliv. 5 (2008) 102–107. https://doi.org/10.2174/156720108783954851.

[32] V.P. Costa, M.E.M. Braga, C.M.M. Duarte, C. Alvarez-Lorenzo, A. Concheiro, M.H. Gil, H.C. de Sousa, Anti-glaucoma drug-loaded contact lenses prepared using supercritical solvent impregnation, J. Supercrit. Fluids. 53 (2010) 165–173. https://doi.org/10.1016/j.supflu.2010.02.007.

[33] Y. Masmoudi, L. Ben Azzouk, O. Forzano, J.M. Andre, E. Badens, Supercritical impregnation of intraocular lenses, J. Supercrit. Fluids. 60 (2011) 98–105. https://doi.org/10.1016/j.supflu.2011.08.014.

[34] Y. Yokozaki, J. Sakabe, B. Ng, Y. Shimoyama, Effect of temperature, pressure and depressurization rate on release profile of salicylic acid from contact lenses prepared by supercritical carbon dioxide impregnation, Chem. Eng. Res. Des. 100 (2015) 89–94. https://doi.org/10.1016/j.cherd.2015.05.008.

[35] Y. Yokozaki, J. Sakabe, Y. Shimoyama, Enhanced impregnation of hydrogel contact lenses with salicylic acid by addition of water in supercritical carbon dioxide, Chem. Eng. Res. Des. 104 (2015) 203–207. https://doi.org/10.1016/j.cherd.2015.08.007.

[36] A. Bouledjouidja, Y. Masmoudi, M. Sergent, V. Trivedi, A. Meniai, E. Badens, Drug loading of foldable commercial intraocular lenses using supercritical impregnation, Int. J. Pharm. 500 (2016) 85–99. https://doi.org/10.1016/j.ijpharm.2016.01.016.

[37] A. Bouledjouidja, Y. Masmoudi, M. Sergent, E. Badens, Effect of operational conditions on the supercritical carbon dioxide impregnation of anti-inflammatory and antibiotic drugs in rigid commercial intraocular lenses, J. Supercrit. Fluids. 130 (2017) 63–75. https://doi.org/10.1016/j.supflu.2017.07.015.

[38] A. Bouledjouidja, Y. Masmoudi, Y. Li, W. He, E. Badens, Supercritical impregnation and optical characterization of loaded foldable intraocular lenses using supercritical fluids, J. Cataract Refract. Surg. 43 (2017) 1343–1349. https://doi.org/10.1016/j.jcrs.2017.07.033.

[39] Y. Yokozaki, Y. Shimoyama, Loading of vitamin E into silicone hydrogel by supercritical carbon dioxide impregnation toward controlled release of timolol maleate, J. Supercrit. Fluids. 131 (2018) 11–18. https://doi.org/10.1016/j.supflu.2017.08.010.

[40] V.P. Costa, M.E.M. Braga, J.P. Guerra, A.R.C. Duarte, C.M.M. Duarte, E.O.B. Leite, M.H. Gil, H.C. de Sousa, Development of therapeutic contact lenses using a supercritical solvent impregnation method, J. Supercrit. Fluids. 52 (2010) 306–316. https://doi.org/10.1016/j.supflu.2010.02.001.

[41] C. Wertheimer, S. Kassumeh, N.P. Piravej, O. Nilmayer, C. Braun, C. Priglinger, N. Luft, A. Wolf, W.J. Mayer, S.G. Priglinger, K.H. Eibl-Lindner, The Intraocular Lens as a Drug Delivery Device: In Vitro Screening of Pharmacologic Substances for the Prophylaxis of Posterior Capsule Opacification, Investig. Opthalmology Vis. Sci. 58 (2017) 6408. https://doi.org/10.1167/iovs.17-22555.
[42] A.-Z. Chen, L. Li, S.-B. Wang, C. Zhao, Y.-G. Liu, G.-Y. Wang, Z. Zhao, Nanonization of methotrexate by solution-enhanced dispersion by supercritical CO2, J. Supercrit. Fluids. 67 (2012) 7–13. https://doi.org/10.1016/j.supflu.2012.03.004.
[43] A. Chen, T. Dang, S. Wang, N. Tang, Y. Liu, W. Wu, The in vitro and in vivo anti-tumor effects of MTX-Fe3O4-PLLA-PEG-PLLA microspheres prepared by suspension-enhanced dispersion by supercritical CO2, Sci. China Life Sci. 57 (2014) 698–709. https://doi.org/10.1007/s11427-014-4680-8.
[44] A.-Z. Chen, L. Li, S.-B. Wang, X.-F. Lin, Y.-G. Liu, C. Zhao, G.-Y. Wang, Z. Zhao, Study of Fe3O4–PLLA–PEG–PLLA magnetic microspheres based on supercritical CO2: Preparation, physicochemical characterization, and drug loading investigation, J. Supercrit. Fluids. 67 (2012) 139–148. https://doi.org/10.1016/j.supflu.2012.04.009.
[45] A. Bertucco, G. Vetter, High pressure process technology: fundamentals and applications, Elsevier, 2001.
[46] M. Champeau, J.M. Thomassin, T. Tassaing, C. Jérôme, Drug loading of polymer implants by supercritical CO 2 assisted impregnation: A review, J. Controlled Release. 209 (2015) 248–259. https://doi.org/10.1016/j.jconrel.2015.05.002.
[47] E. Carretier, E. Badens, P. Guichardon, O. Boutin, G. Charbit, Hydrodynamics of Supercritical Antisolvent Precipitation: Characterization and Influence on Particle Morphology, Ind. Eng. Chem. Res. 42 (2003) 331–338. https://doi.org/10.1021/ie020439v.
[48] R.W. Korsmeyer, N.A. Peppas, Effect of the morphology of hydrophilic polymeric matrices on the diffusion and release of water soluble drugs, J. Membr. Sci. 9 (1981) 211–227. https://doi.org/10.1016/S0376-7388(00)80265-3.
[49] P.L. Ritger, N.A. Peppas, A simple equation for description of solute release II. Fickian and anomalous release from swellable devices, J. Controlled Release. 5 (1987) 37–42. https://doi.org/10.1016/0168-3659(87)90035-6.
[50] G. Cleary, D.J. Spalton, J.J. Zhang, J. Marshall, In vitro lens capsule model for investigation of posterior capsule opacification, J. Cataract Refract. Surg. 36 (2010) 1249–1252. https://doi.org/10.1016/j.jcrs.2010.05.006.
[51] A.J.O. Smith, J.A. Eldred, I.M. Wormstone, Resveratrol Inhibits Wound Healing and Lens Fibrosis: A Putative Candidate for Posterior Capsule Opacification Prevention, Invest. Ophthalmol. Vis. Sci. 60 (2019) 3863–3877. https://doi.org/10.1167/iovs.18-26248.
[52] K. Shi, L. Feng, L. He, H. Li, Thermodynamic modeling of the supercritical CO2 impregnation process for the preparation ibuprofen/polymethylmethacrylate composite, J. Taiwan Inst. Chem. Eng. 78 (2017) 471–476. https://doi.org/10.1016/j.jtice.2017.05.033.
[53] I. Pasquali, R. Bettini, Are pharmaceutics really going supercritical?, Int. J. Pharm. 364 (2008) 176–187. https://doi.org/10.1016/j.ijpharm.2008.05.014.
[54] I. Kikic, F. Vecchione, Supercritical impregnation of polymers, Curr. Opin. Solid State Mater. Sci. 7 (2003) 399–405. https://doi.org/10.1016/j.cossms.2003.09.001.
[55] I.M. Wormstone, S. Tamiya, I. Anderson, G. Duncan, TGF-beta2-induced matrix modification and cell transdifferentiation in the human lens capsular bag, Invest. Ophthalmol. Vis. Sci. 43 (2002) 2301–2308.
[56] C.M. Wertheimer, M. Shajari, T. Kohnen, A. von Studnitz, S. Kassumeh, S. Dimitriou, R. Lieberz, I. Hakim, S.G. Priglinger, W.J. Mayer, Comparison of fibrotic response in the human lens capsular bag after femtosecond laser–assisted cataract surgery and conventional phacoemulsification, J. Cataract Refract. Surg. 44 (2018) 750–755. https://doi.org/10.1016/j.jcrs.2018.01.035.
[57] A. Tiwari, J. Ram, M. Luthra-Guptasarma, Targeting the fibronectin type III repeats in tenascin-C inhibits epithelial-mesenchymal transition in the context of posterior capsular opacification, Invest. Ophthalmol. Vis. Sci. 56 (2014) 272–283. https://doi.org/10.1167/iovs.14-14934.
[58] L.J. Tang, C.L. Gu, P. Zhang, Intraocular lymphoma, Int. J. Ophthalmol. 10 (2017) 1301–1307. https://doi.org/10.18240/ijo.2017.08.19.
[59] K. Julian, B.-J. Langner Wegscheider, A. Haas, M.D. De Smet, Intravitreal methotrexate in the management of presumed tuberculous serpiginous-like choroiditis, Retina Phila. Pa. 33 (2013) 1943–1948. https://doi.org/10.1097/IAE.0b013e318285cdbe.
[60] K. Ghasemi Falavarjani, S. Golabi, A. Hadavandkhani, Effect of Intravitreal Injection of Methotrexate on Human Corneal Endothelial Cells, Cornea. 35 (2016) 217–219. https://doi.org/10.1097/ICO.0000000000000700.

Tables

Table 1: Repeatability of methotrexate impregnation in Bausch&Lomb IOLs (+23.0D) with pure supercritical CO_2 at 25 MPa and 308 K during 240 min

Sample	m_{imp}* (µg)	DL** ± 0.03 ($\mu g_{drug}.mg^{-1}_{IOL}$)
1	8.1	0.43
2	8.5	0.47
3	7.8	0.43
Average ± SD	8.1 ± 0.4	0.44 ± 0.02

Experimental errors: * ± 0.5 µg; ** ± 0.03 $\mu g_{drug}.mg^{-1}_{IOL}$

Table 2: Drug loading and durations for complete release from IOLs (+20.0D) depending on operating conditions of impregnation

Sample	Pressure (MPa)	Duration (min)	m_{imp}* (µg)	DL** ($\mu g_{drug}.mg^{-1}_{IOL}$)	$t_{release}$*** (days)	Release kinetic parameters		
						K (d^{-n})	*n*	R^2
Without co-solvent								
1	8	30	9.6	0.53	100	0.10	0.48	0.93
2	8	240	13.5	0.75	117	0.08	0.50	0.98
3	25	240	8.4	0.43	87	0.07	0.53	0.96
With co-solvent								
4	8	30	10.8	0.59	110	0.10	0.50	0.92
5	8	240	11.2	0.62	109	0.13	0.40	0.91
6	25	240	9.2	0.5	98	0.04	0.60	0.93

Experimental errors: * ± 0.5 µg; ** ± 0.03 $\mu g_{drug}.mg^{-1}_{IOL}$; *** ± 7 days

Figures

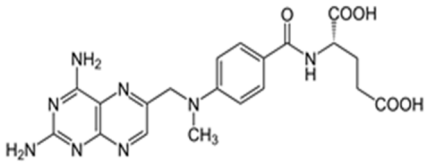

Fig. 1. Chemical structure of methotrexate

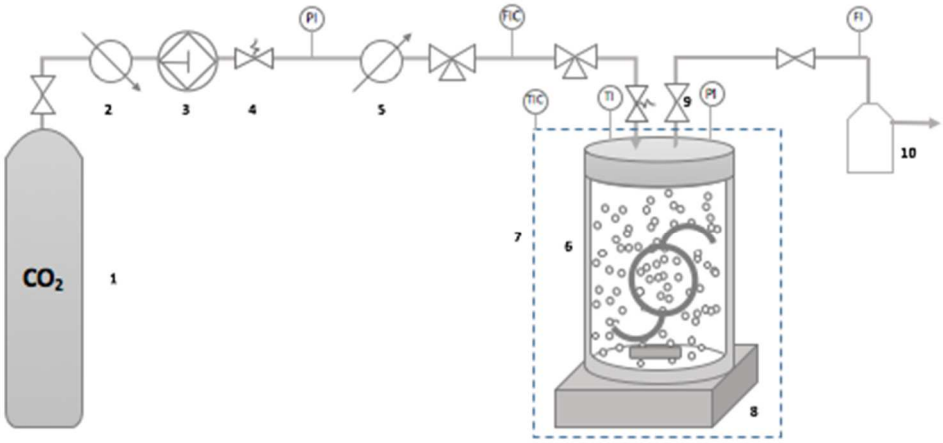

Fig. 2. Supercritical impregnation set-up: (1) CO_2 cylinder, (2) cooling bath, (3) high pressure liquid pump, (4) safety valve, (5) heating bath, (6) high pressure cell, (7) thermostat bath, (8) magnetic bar, (9) depressurization valve, (10) solvent trap.

a)

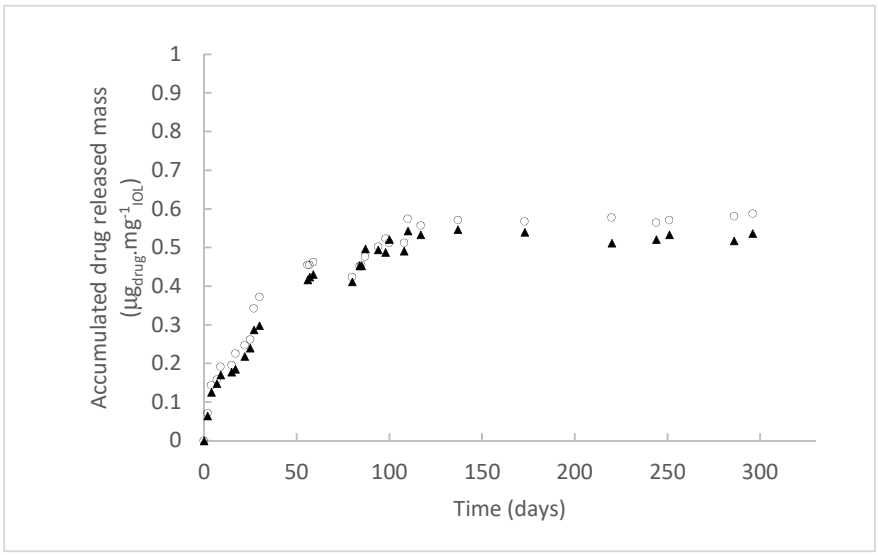

b)

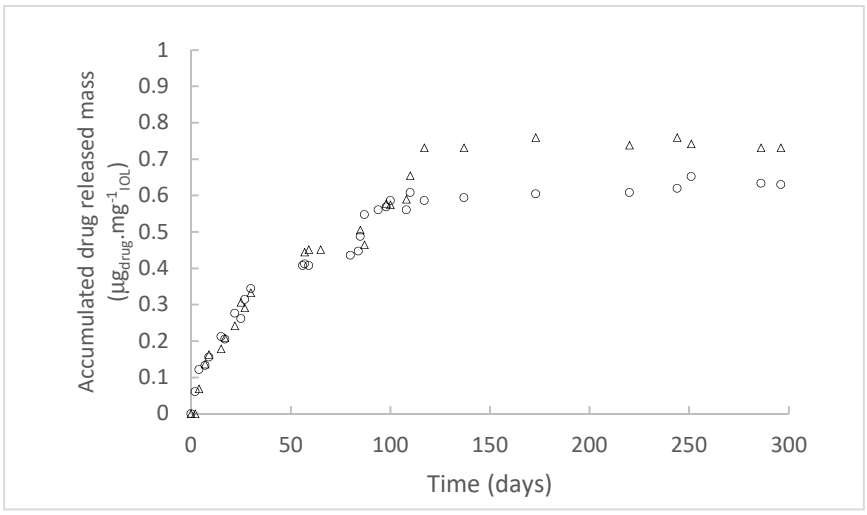

c)

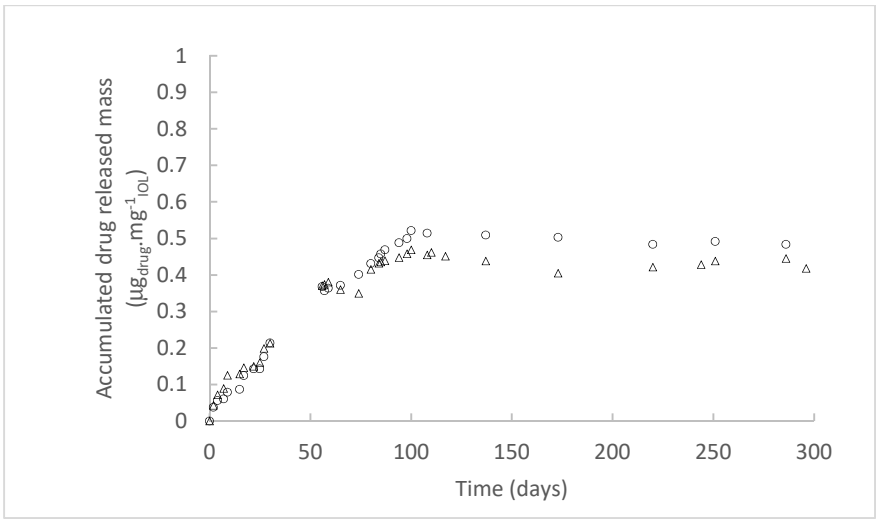

Fig. 3: Accumulated drug release from Bausch&Lomb IOLs (+20.0D) impregnated with methotrexate Δ without co-solvent and ○ with ethanol 5 mol% at 308 K and a) 8 MPa during 30 min, b) 8 MPa during 240 min and c) 25 MPa during 240 min.

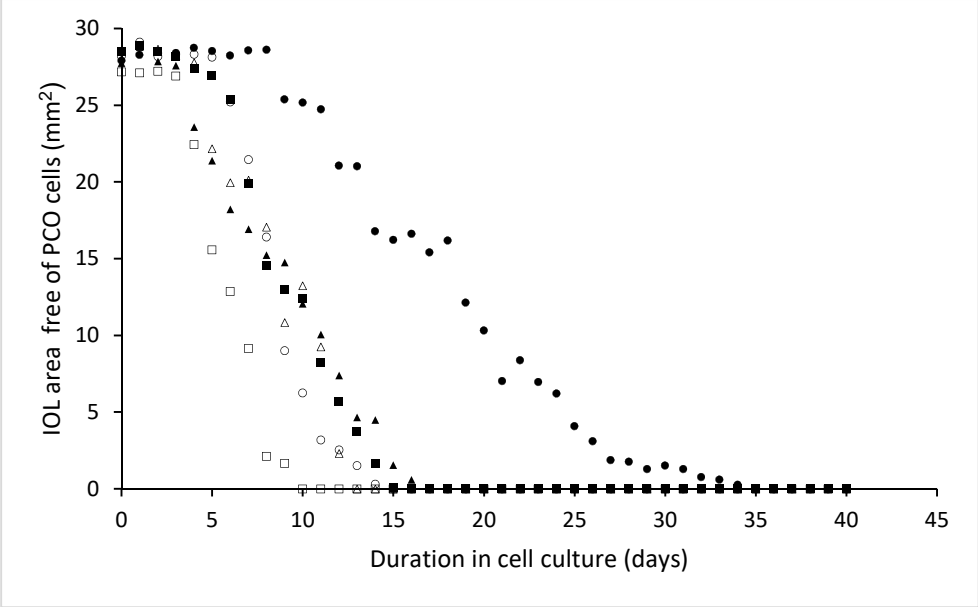

Fig. 4: The growth of lens epithelial cells as a marker for PCO on the posterior capsule is presented as IOL area free of cells in methotrexate loaded IOLs compared to control IOLs for three pairs of eyes. (•, ▲ and ▪) Methotrexate loaded IOLs and (○, △ and ▫) control IOLs (1, 2 and 3 respectively).

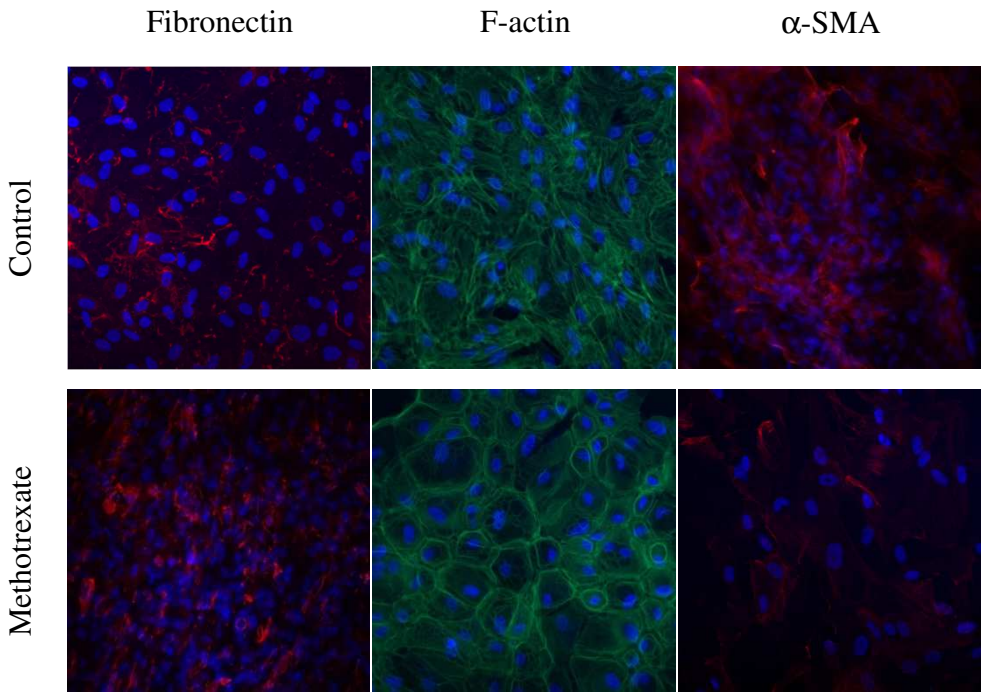

Fig. 5 Immunofluorescence images of fibronectin, F-actin and α-SMA marked proteins on the posterior capsule of capsular bags.

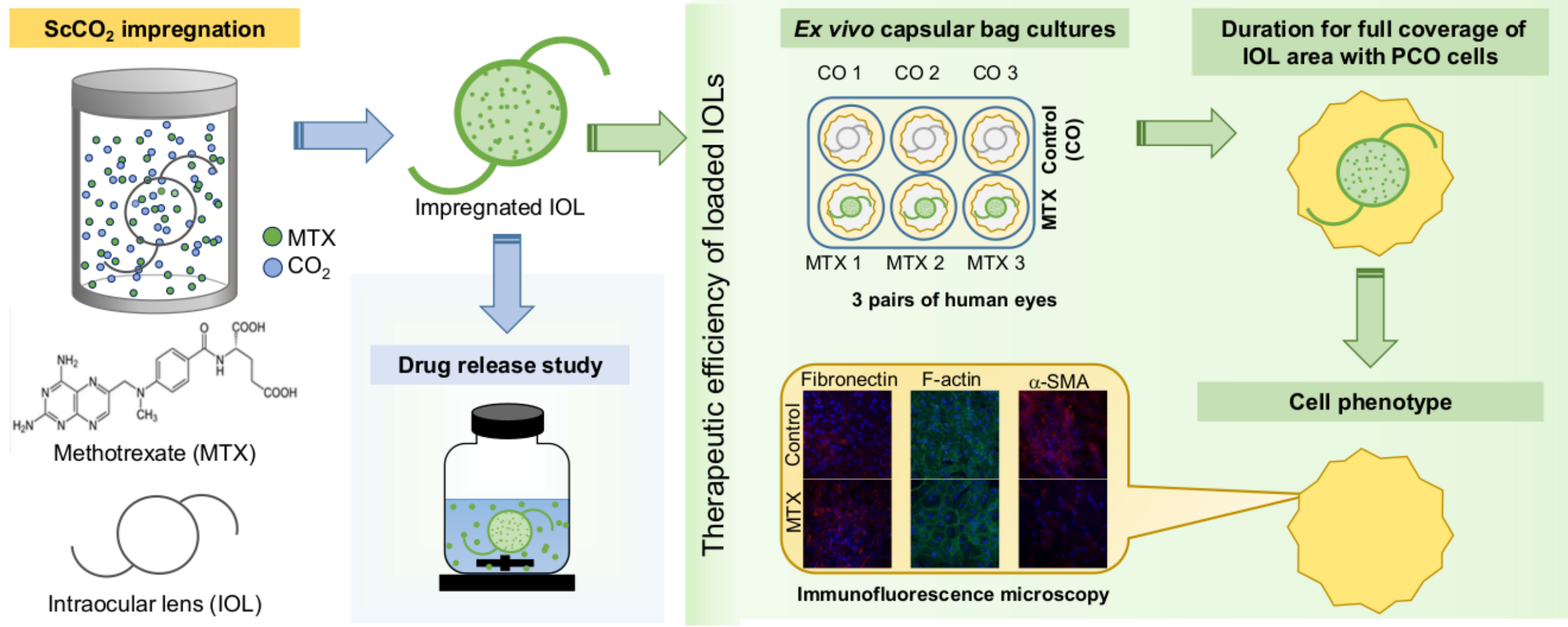
ScCO2 impregnation
MTX
CO2
Impregnated IOL
Methotrexate (MTX)
Intraocular lens (IOL)
Drug release study
Therapeutic efficiency of loaded IOLs
Ex vivo capsular bag cultures
CO 1
CO 2
CO 3
Control (CO)
MTX
MTX 1
MTX 2
MTX 3
3 pairs of human eyes
Duration for full coverage of IOL area with PCO cells
Cell phenotype
Fibronectin
F-actin
α-SMA
Control
MTX
Immunofluorescence microscopy